Tunable micro-electromechanical grating in silicon

Yves-Alain Peter, Fatou Binetou Koné, Jonathan Masson, Nicolas Godbout
École Polytechnique de Montréal, Engineering Physics Department
Montréal (Québec) H3C 3A7, CANADA
yves-alain.peter@polymtl.ca

ABSTRACT

In this paper, we propose a solution for simple, fast and easily controllable way of tuning silicon gratings using Micro Electro Mechanical Systems (MEMS) to deform the grating itself. Basically the idea is to deform mechanically a silicon grating using electrostatic actuators, enabling pitch tuning over a large proportion (more than 50% is easily achievable with our approach). Moreover we can change the spacing of individual layers within the grating. A theoretical analysis and numerical simulations are presented and a first prototype is fabricated. Bragg gratings, springs and actuators are realized by silicon micro/nano machining on a silicon platform enabling full integration and passive alignment of all optical components. Applications range from ultra-sensitive displacement sensors, to telecommunications and biology.

Keywords: MEMs, grating, silicon, Fabry-Perot, Bragg, DRIE

1. INTRODUCTION

Gratings play an important role in optical systems and devices. Diffraction gratings are used as multiplexers/demultiplexers (MUX/DEMUX) in wavelength division multiplexing (WDM) systems [1]. They are also widely used in spectroscopy [2]. Fiber Bragg gratings, used as selective reflectors, are a key element in optical fiber communication [3, 4]. Gratings are usually static and their properties are defined once during fabrication. Dynamically tuning the optical properties of gratings is highly interesting. It has been a driving motivation for research for several years. Fiber Bragg gratings have been tuned thermally and mechanically [4, 5]. For example, a tunable fiber laser using a stretchable Bragg grating has been demonstrated by Pan [6], but exhibit a limited tuning range of 11nm only. Moreover, no simple, fast, easily controllable way of tuning gratings has been demonstrated to date. We propose a solution for simple, fast and easily controllable way of tuning silicon gratings using Micro Electro Mechanical Systems (MEMS). MEMS have been previously used to tune external cavity lasers (ECLs). Tuning is achieved through a rotation of either the grating or a mirror associated with the grating. While controlled rotation of out-of-plane elements is used in existing MEMS based ECLs [7], a simpler solution is to deform the grating itself. Basically the idea is to deform mechanically a silicon grating using electrostatic actuators. Diffraction gratings using MEMS are widely used for displays [8]. It is a well known device commercialized by Silicon Light Machines under the name “Grating Light Valve” [9]. In this case, the grating is displaced as a whole. What we propose here is going well beyond this type of displacement/tuning. We want to deform the grating itself using MEMS, enabling pitch tuning over a large proportion (more than 50% is easily achievable with our approach). Moreover we can change the spacing of individual layers within the grating. We recently demonstrated pitch tuning on a planar diffractive grating in silicon [10]. The grating has been structured in a thin layer of single crystalline silicon. Parallel springs were attached to the grating and deformed by electrostatic comb drive actuators. Here, we present the concept and fabrication of deep (80μm) vertical silicon Bragg gratings tuned by parallel springs and electrostatic micro actuators. Bragg gratings, springs and actuators are realized by silicon micro/nano machining on a silicon platform enabling full integration and passive alignment of all optical components. Two static vertical silicon gratings forming a tunable Fabry-Pérot cavity has been previously reported [11]. Our approach has added versatility since each individual layer of the grating can be tuned. Applications range from ultra-sensitive displacement sensors, to telecommunications and biology.

Optomechatronic Micro/Nano Devices and Components II, edited by Yoshitada Katagiri,
Proc. of SPIE Vol. 6376, 637604, (2006) · 0277-786X/06/$15 · doi: 10.1117/12.690773

2. THEORETICAL ANALYSIS AND NUMERICAL SIMULATIONS

The very high refractive index contrast between silicon and air generates Bragg reflectors with very interesting properties. The reflection coefficient for each interface is approximately 25%. A structure with four periods reflects 99,99% of the light. One can therefore fabricate highly reflective Bragg gratings of length less than 10 microns, which is impossible using fiber Bragg gratings. This enables the fabrication of devices that are impractical or impossible to realize directly in optical fibers, with the added advantage of tunability.

2.1. Theoretical analysis

We use the transfer matrix method [12] to simulate the transmitted light of wavelength λ across a grating or a Fabry-Pérot (FP) type filter made of two gratings separated by an air gap. Each layer of silicon and air has its own corresponding characteristic matrix. If we consider the angle of incidence of the light normal to the surface, then the characteristic matrix M_j for one layer is [13]:

$$M_j = \begin{Bmatrix} \cos\delta_j & i/n_j \sin\delta_j \\ in_j \sin\delta_j & \cos\delta_j \end{Bmatrix}, \tag{1}$$

where

$$\delta_j = \frac{2\pi n_j d_j}{\lambda} . \tag{2}$$

Each layer j is defined by its thickness d_j and its refractive index n_j. The total transfer matrix for N layers is given by the product of the characteristic matrices of each layer

$$M = \begin{Bmatrix} m_{11} & im_{12} \\ im_{21} & m_{22} \end{Bmatrix} = \prod_{j=1}^{N} M_j . \tag{3}$$

The transmittance of the total layers is

$$T = \tau\tau^* , \tag{4}$$

where

$$\tau = \frac{2}{m_{11} + im_{12} + im_{21} + m_{22}} . \tag{5}$$

2.2. Numerical simulations

Using the transfer matrix method, it is straightforward to calculate the transmission and reflection through vertical silicon gratings. Figure 1 shows a schematic drawing of such a grating. The grating is made of material 1 with thickness d and refractive index n_1, and material 2 with thickness e and refractive index n_2. For simulation purposes, we calculate the transmitted and reflected coefficients for each layer or wall.

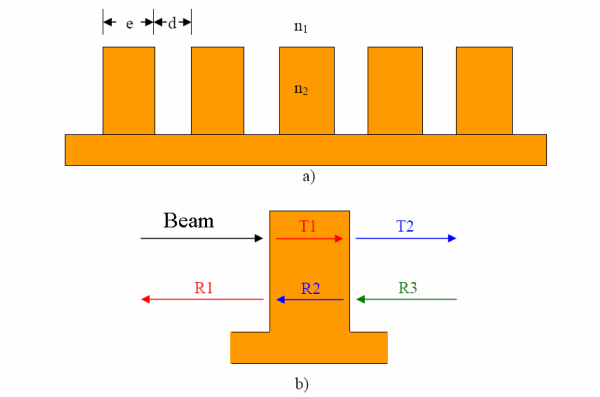

Fig. 1. Schematic drawing of a vertical grating. a) Grating made of material 1 with thickness d and refractive index n_1, and material 2 with thickness e and refractive index n_2. b) Transmitted and reflected coefficients for each layer or wall.

In our case, we will use air as material 1 and silicon as material 2. At a wavelength λ =1550nm, n_{Si}=3.45 and n_{air}=1. We have the following relation between the wavelength and the thickness of each layer:

$$\Lambda = \frac{N\lambda}{4n} \tag{6}$$

At the first order (N=1), we have a silicon thickness of Λ_{Si}=112nm and an air gap of Λ_{air}=388nm. However, we can have the dimensions be a multiple of higher order N=(2m+1) Λ_{Si}.

2.2.1. Static gratings

Thanks to the high refractive index contrast between silicon and air (the reflection coefficient for each interface is approximately 25%), a structure with four periods reflects 99,99% of the light. Figure 2 shows the normalized reflectance versus wavelength of three different gratings with respectively 1, 2 and 5 layers or walls. The thicknesses are chosen for the 51storder for silicon and 11th order for air, i.e., silicon thickness: 5.71 µm and air thickness: 4.26 µm.

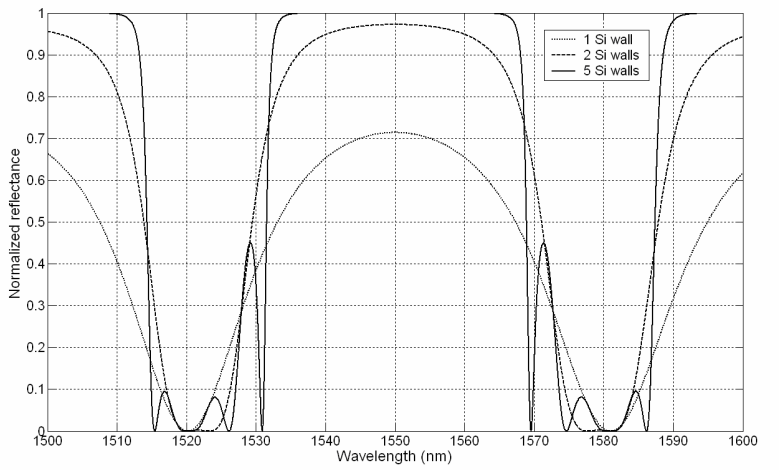

Fig. 2. Normalized reflectance versus wavelength of three different gratings with respectively 1, 2 and 5 layers or walls. Silicon thickness: 2.35µm and air thickness: 8.15µm (21st order).

A consequence of the high refractive index contrast between silicon and air is a wide bandwidth of the grating for low order gratings. Figure 3 shows the normalized reflectance of a three layers (walls) grating for four different orders of silicon: 1st, 21st, 51st and 101st. The order of the air layers is kept constant at 11 st. Note that the corresponding silicon thicknesses are: d_{Si}=112nm for the first order, d_{Si}=2.35μm for the 21st order, d_{Si}=5.71μm for the 51st order, and d_{Si}=11.31μm for the 101st order. At the first order, the bandwidth is so large, that the normalized reflectance is close to 1 over the 1500nm-1600nm range. With increasing orders, the bandwidth decreases down to around 20nm for the 101st order. Note that side loops are also coming closer to the central wavelength.

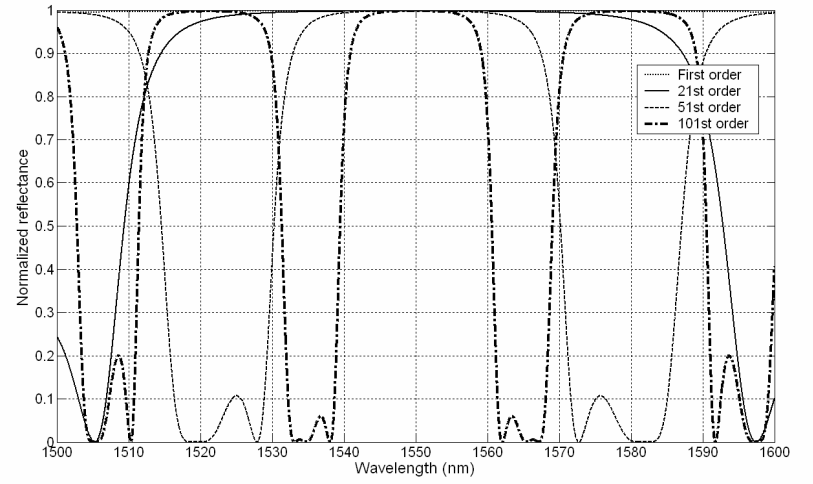

Fig. 3. Normalized reflectance versus wavelength for a three layer grating with four different orders: 1st, 21st, 51st and 101st.

2.2.2. Tunable gratings

Considering a grating with three layers (or walls) at the 51st order, let see how the displacement of the central layer influences the reflectance spectrum. Figure 4 shows the normalized reflectance of such a grating with the central wall being displaced by 0μm, 1μm, 2μm, and 4μm. For the 51st order, we have d_{Si}=5.71μm and d_{air}=19.79μm. We see that the reflectance spectrum is degraded with increasing displacement, without a clear relation with the bandwidth or amplitude.

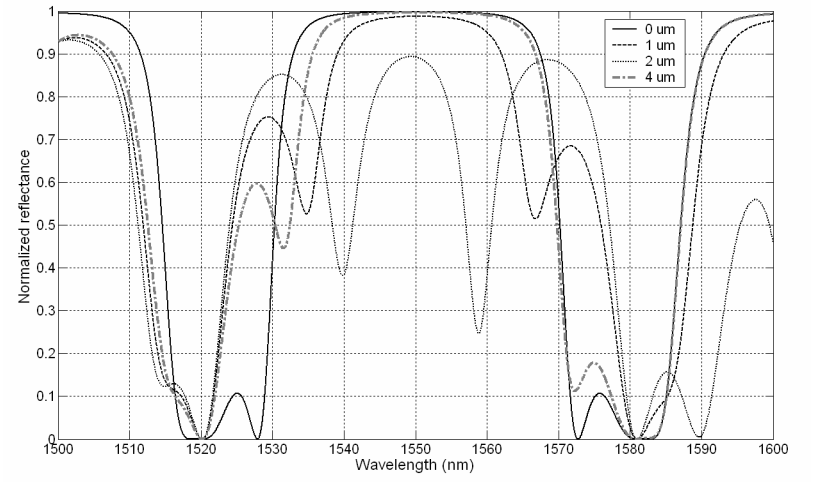

Fig. 4. Normalized reflectance versus wavelength for a three layers grating with thicknesses corresponding to the 51st order. The central layer is displaced by 0μm, 1μm, 2μm, and 4μm.

Another way of tuning the response of the grating can be done by compressing the grating like an accordion. Basically, this means a homogenous shrink of the air gaps. As expected, this leads to a shift of the reflected wavelength, as can be shown in Fig. 5. In this figure, we see the normalized reflectance versus wavelength for a three layer grating at the 51st order with outside layers moving equally by 0μm, 0.12μm, and 0.24μm.

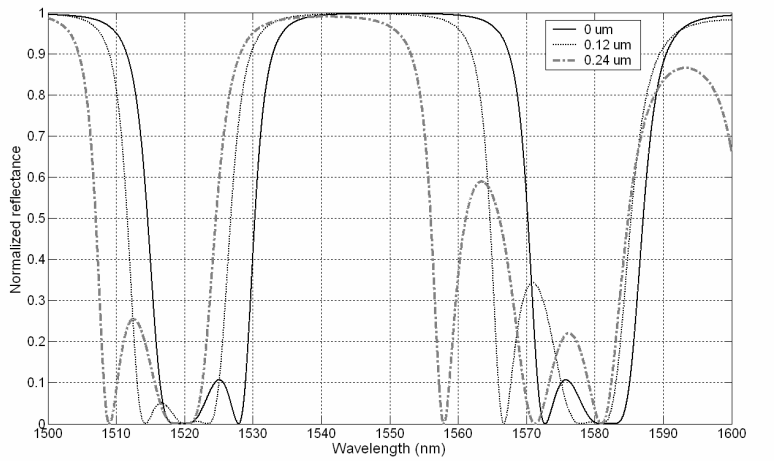

Fig. 5. Normalized reflectance versus wavelength for a three layers grating with thicknesses corresponding to the 51st order. The outside layers are equally displaced by 0μm, 0.12μm, and 0.24μm.

2.2.3. Fabry-Pérot cavity

An interesting device that can benefit from the tunability of the gratings is the Fabry-Pérot cavity. It consists of two reflectors separated by an air gap of m λ/2, where m is an integer. In such a configuration, we can use our tunable gratings as reflectors. The Fabry-Pérot cavity can be tuned by changing the air gap between the two reflectors as is usually done, but also by tuning the gratings themselves.

Let's take a Fabry-Pérot cavity with two three-layers gratings as reflectors and a gap of λ (m=2). Figure 6 shows the normalized transmittance of the Fabry-Pérot cavity. The inset is a close up view of the peaks for three different orders of the gratings: 1st, 23rd and 41st. Here, we see that increasing the order of the grating will produce a narrower bandwidth. However, increasing the order too much (see e.g. 41st order) will bring the side loops closer to the central wavelength.

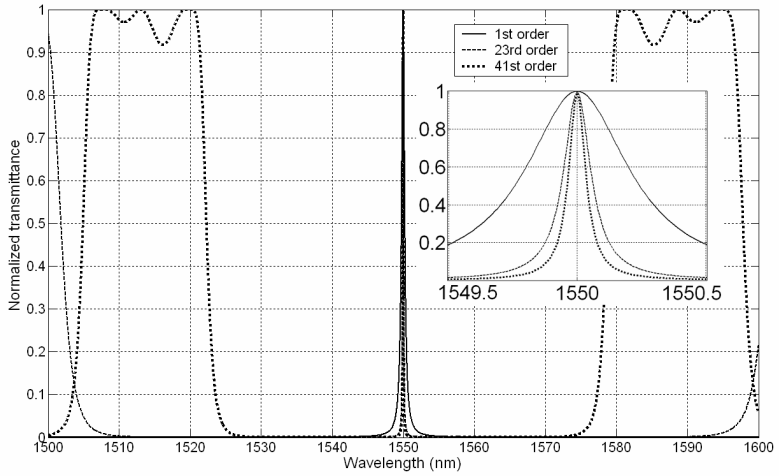

Fig. 6. Normalized transmittance versus wavelength of a Fabry-Pérot cavity with two three-layers gratings as reflectors and a gap of λ (m=2). Inset: close up view of the peaks for three different orders of the gratings: 1st, 23rd and 41st.

The peak transmittance wavelength can be tuned by changing the air spacing between the two gratings. In Fig. 7, the air gap between the two gratings is changed from 1.49μm to 1.61μm. Silicon layers are in the 21st order, air gaps within the gratings are in the 5th order and the Fabry-Pérot cavity air gap is in the 2nd order (m=2). By moving a single layer within one of the gratings, it is possible to change the amplitude of the transmittance. In Fig. 6, we see how the displacement of 230nm of a single layer generates 3dB attenuation.

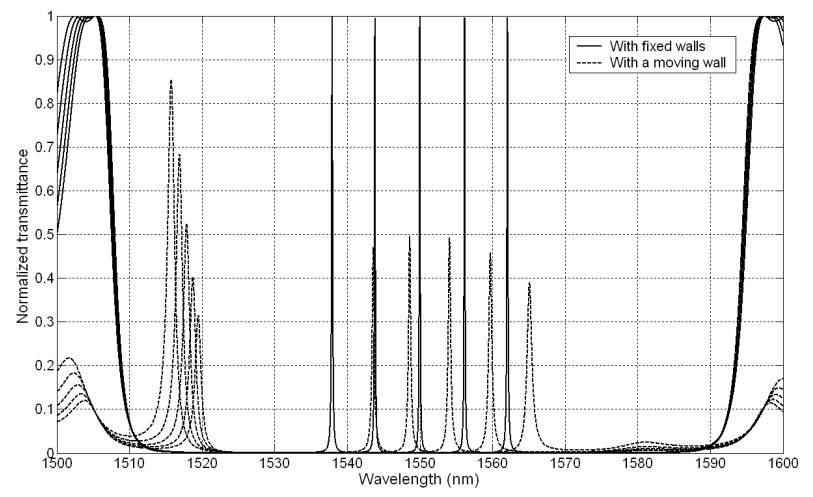

Fig. 7. Plain line: normalized transmittance versus wavelength of a Fabry-Pérot cavity made of two three-layers gratings as reflectors and a varying gap from 1.49μm to 1.61μm. Dotted line: same Fabry-Pérot cavity with a single layer (wall) within one of the gratings displaced by 230nm.

We have seen in this section how adding tunability (grating order and/or deformation) to vertical silicon gratings generates interesting effects in terms of wavelength tunability, bandwidth and attenuation.

3. FABRICATION

In this section, we will describe a fabrication process used to demonstrate the effect of individual layer displacement in a silicon vertical grating deformed with micro actuators. The schematic of the device is shown in Fig. 8.

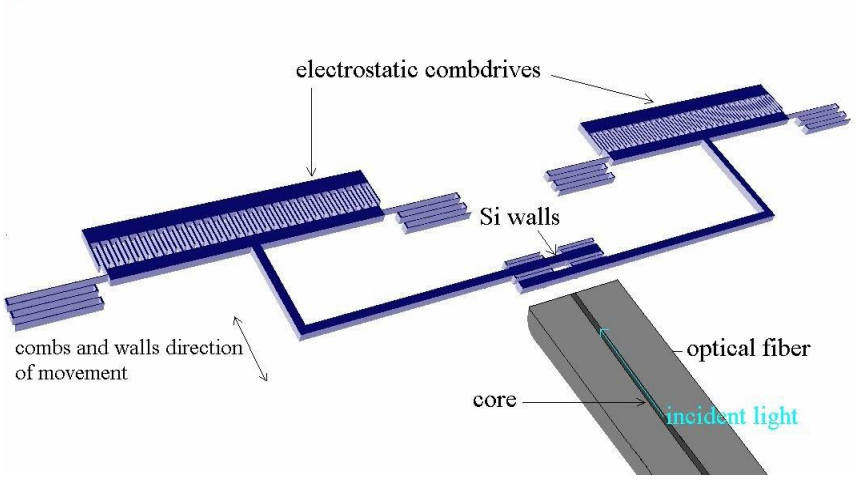

Fig. 8. Schematic drawing of the complete prototype including grating, comb drive actuators, springs and optical fiber.

We designed a simple two layer grating, whose layers or walls are connected to comb drives actuators with mechanical springs. Applying a voltage on the comb drives actuators will move the walls and tune the grating optical response. An optical fiber is integrated to the platform and passively aligned in grooves fabricated together with the grating and actuators themselves.

The process flow for the microfabrication of the device is shown in Fig. 9. (a) The device is fabricated in a SOI wafer that has a 10µm device layer, 2µm box and 500µm handle. (b) A first lithography step is done to pattern the pads which will be metallized by lift off with a very thin layer of gold. (c) A second lithography step is realized to pattern the device layer comprising all structural components: grating, springs and actuators. (d) Etching is done by Deep Reactive Ion Etch in an Inductively Coupled Plasma (DRIE ICP). We use Shipley S-1813 photoresist because it provides good lithography resolution up to micron precision and has an excellent dry etch selectivity (1: 33, experimental), which is sufficient for the depths that we want to reach in this device. To smooth the scalloping produced by the deep etch and obtain optically efficient surfaces, the parameters have to be optimized, therefore, low ICP and RF powers were used (350W and 10W respectively) with very low etch times and even lower passivation times (5s and 3s respectively). Moreover, a slight amount of O_2 was introduced during the etching step. After etching, a thermal oxidation is done to help smooth even more the vertical surfaces and reduce the scalloping effects. This oxide layer will be removed during the final release. (e) A third photolithography step is executed to pattern the optical fiber grooves: (f) first the oxide at the bottom of the grooves is removed by Reactive Ion Etching (RIE) and (g) then 51µm of the handle are etched so that the entire core of the fiber will face the reflectors. (h) Finally, the structures are released using a vapor HF system (Idonus) that operates with concentrated HF (49%) at ambient temperature on a slightly heated (30-40ºC) substrate to avoid stiction.

Fig. 9. Process flow for the microfabrication of the tunable vertical silicon grating.

A fabricated device is shown in Fig. 10. In this photograph, the optical fiber groove has not been etched away.

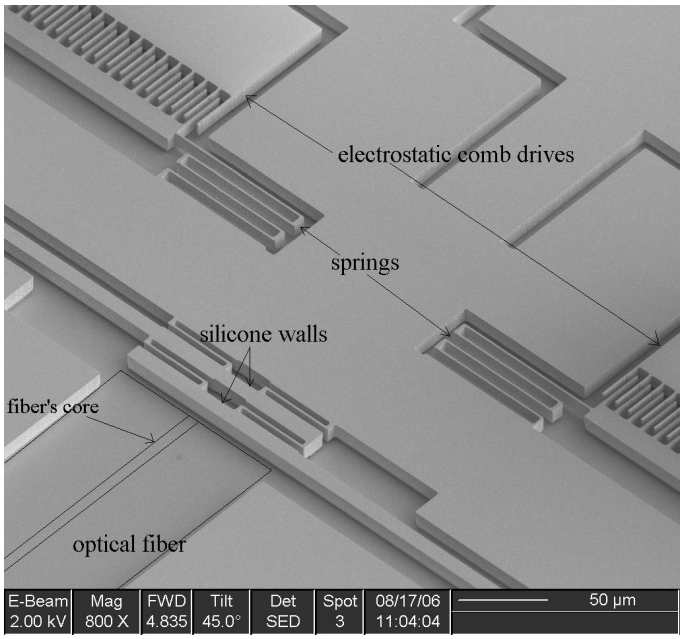

Fig. 10. SEM photograph of one fabricated device.

CONCLUSION

We proposed, designed simulated and fabricated a tunable micro-electromechanical grating in silicon. In particular, we have described the influence on the optical response of the grating from varying: number of layers and from the order of the grating. In addition, we have shown how the displacement of a single layer will affect the reflectance of the grating and how the homogenous deformation of the grating (accordion compression) will shift its central reflectance wavelength. A particular application on a tunable Fabry-Pérot cavity has been simulated to demonstrate variable attenuation through a single layer displacement within one of the two gratings of the cavity. A process flow has been established and first prototypes have been microfabricated.

ACKNOWLEDGEMENTS

This work was supported by the Natural Sciences and Engineering Research Council of Canada under the Discovery Program.

REFERENCES

1. J.-P. Laude and J.M. Lerner, “Wavelength division multiplexing/demultiplexing (WDM) using diffraction gratings,” *Proceedings of the SPIE*, Vol. 503, pp. 22-28, 1984.
2. E.G. Loewen, “Diffraction gratings for spectroscopy,” *Journal of Physics E (Scientific Instruments)*, Vol. 3, No. 12, pp. 953-61, 1970.
3. A. Othonos, “Fiber Bragg gratings,” *Rev. Sci. Instrum.*, Vol. 68, No. 12, pp. 4309-4341, 1997.
4. R. Kashyap, “Fiber Bragg gratings,” Academic Press, 1999.
5. K.O. Hill and G. Meltz, “Fiber Bragg grating technology fundamentals and overview,” *Journal of Lightwave Technology*, Vol. 15, No. 8, pp. 1263-1276, 1997.

6. J. Pan,Y. Shi, T. Zhu,“Continuously tunable high power fiber lasers with 11 nm tunability,” *Optical Fiber Communication Conference*, Vol. 2, pp.199-201, 1999.
7. D. Anthon, J.D. Berger, J. Drake, S. Dutta, A. Fennema, J.D.Grade, S. Hrinya, F. Ilkov, H. Jerman, D. King, H. Lee, A. Tselikov, K. Yasumura, “External cavity diode lasers tuned with silicon MEMS,” *Optical Fiber Communication Conference*, Anaheim, CA, March 17-22, pp. 97-98, 2002.
8. 0. Solgaard, E S. A. Sandejas, and D. M. Bloom, “Deformable grating optical modulator,” *Optics Letters*, Vol. 17, No. 9, pp. 688-690, 1992.
9. D.M. Bloom, “The Grating Light Valve: revolutionizing display technology,” *Proceedings of the SPIE*, Vol. 3013, pp. 165-171, 1997.
10. M. Tormen, Y.-A. Peter, Ph. Niedermann, A. Hoogerwerf, R. Stanley, "Deformable MEMS grating for wide tunability and high operating speed," *Journal of Optics A: Pure and Applied Optics*, Vol. 8, No. 7, pp. S337-40, 2006.
11. A. Lipson et al., “Low-loss one-dimensional photonic bandgap filter in (110) silicon,” *Optics Letters*, Vol. 31, No. 3, 2006.
12. H. Kogelnik and T. Li, “Laser beams and resonators,” *Applied Optics*, Vol. 5, No. 10, pp. 1550-1567, 1966.
13. S. Weidong, L. Xiangdong, H. Biqin, Z. Yong, L. Xu, G. Peifu, “Analysis on the tunable optical properties of MOEMS filter based on Fabry–Perot Cavity,” *Optics Communications,* Vol. 239, pp. 153–160, 2004.